

## NUMERICAL SIMULATION OF FLOW AND POLLUTION DISPERSION OVER OBSTACLES IN COMPLEX TERRAIN

K. Kozel<sup>1)</sup>, T. Bodnár<sup>1)</sup>, E. Gulíková<sup>2)</sup> and V. Píša<sup>2)</sup>

1) Department of technical mathematics, Faculty of mechanical engineering,  
Czech Technical University in Prague

2) ECOPROGRESS a.s., Most

### Introduction

This paper presents some of the results of numerical simulation of flow and pollution dispersion in the proximity of significant terrain obstacles. The mathematical model is based on Reynolds averaged Navier-Stokes equations for incompressible flows. Turbulent closure of the model is obtained by simple algebraic turbulence model. The numerical solution is carried out by the semi-implicit finite-difference scheme. The results of simple tests are presented and summarized. Model sensitivity has been studied with respect to simulated obstacle size and shape.

This study has been motivated by the request to evaluate the possible effect of downwind obstacles on the deposition of wind drifted coal dust. In the presented part of this project we have concentrated our attention to the detailed computation of flow field characteristics in the vicinity of large terrain obstacles. Special attempt has been made to localize the places where the flow is decelerating or recirculating. These flow regimes areas could be critical from the point of view of surface particle deposition.

The complex terrain profile used in this study represents a part of the opencast coal mine where is placed a coal storage. This storage acts as a source of coal dust which is drifted by the wind. The detailed orography profile was obtained by a combination of data from several geographical resources. In order to get maximum of realistic details a laser scan of the terrain was performed and included into the orography profile. The aim of this study is to give both qualitative and quantitative guidelines for the evaluation of the environmental impact of artificial obstacles placed downwind from the coal storage.

### Mathematical Model

The flow in atmospheric boundary is turbulent in most simulations. The fluid motion can be thus described by the Reynolds averaged Navier-Stokes equations (RANS). The non-conservative form of the RANS system is represented by the following equations:

$$u_x + v_y + w_z = 0 \quad (1)$$

$$V_t + uV_x + vV_y + wV_z = -\frac{\nabla p}{\rho} + [KV_x]_x + [KV_y]_y + [KV_z]_z \quad (2)$$

Here  $V = col(u, v, w)$  is the velocity vector,  $p$  is pressure,  $\rho$  is density.

The same form as the momentum equations take also the transport equations for concentration of passive pollutants.

$$C_t^i + uC_x^i + vC_y^i + wC_z^i = \left[ K \frac{C_x^i}{\sigma_{C^i}} \right]_x + \left[ K \frac{C_y^i}{\sigma_{C^i}} \right]_y + \left[ K \frac{C_z^i}{\sigma_{C^i}} \right]_z \quad (3)$$

Here  $C^i$  is the concentration of  $i$ -th pollutant and  $\sigma$  denotes the turbulent Prandtl's number.

The turbulence model is based on the Boussinesq hypothesis on the turbulent diffusion coefficient  $K = \nu + \nu_T$  which is expressed as a sum of molecular and eddy viscosity. Finally the following algebraic turbulence model was used to complete the governing system:

$$K = \nu + \nu_T \quad \text{where} \quad \nu_T = \ell^2 \left[ \left( \frac{\partial u}{\partial z} \right)^2 + \left( \frac{\partial v}{\partial z} \right)^2 \right]^{1/2} \quad (4)$$

The mixing length  $\ell$  is computed according to the following formula:

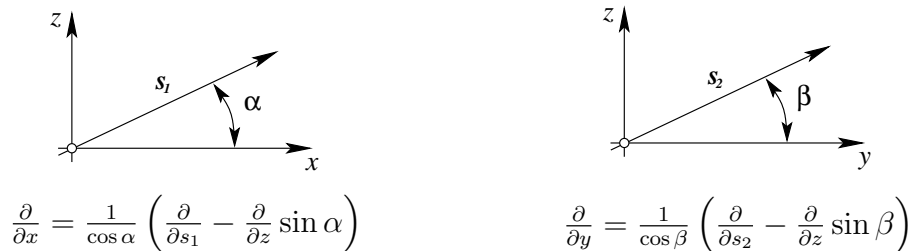
$$\ell = \frac{\varkappa(z + z_0)}{1 + \varkappa \frac{(z+z_0)}{\ell_\infty}} \quad \text{where} \quad \ell_\infty = \frac{27 |V_G| 10^{-5}}{f_c} \quad (5)$$

Here  $f_c = 1.1 \cdot 10^{-4} \text{ms}$  denotes the Coriolis parameter and  $V_G$  is the geostrophic wind velocity at the upper boundary of domain.

## Numerical Solution

### Finite-difference discretization

To discretize the governing system we have constructed the non-orthogonal structured boundary (i.e. terrain) following mesh. Because of the mesh non-orthogonality we have to transform the equations from the  $x - y - z$  coordinates to the mesh-wise directional local coordinate system  $s_1 - s_2 - z$ :



$$\frac{\partial}{\partial x} = \frac{1}{\cos \alpha} \left( \frac{\partial}{\partial s_1} - \frac{\partial}{\partial z} \sin \alpha \right) \quad \frac{\partial}{\partial y} = \frac{1}{\cos \beta} \left( \frac{\partial}{\partial s_2} - \frac{\partial}{\partial z} \sin \beta \right)$$

Figure 1: Local coordinate transformation

To simplify notation of discretized equations we introduce operators of differences. The symbol  $\delta_s$  denotes the central difference with respect to direction  $s$ . Similarly the  $\overrightarrow{\delta}_s, \overleftarrow{\delta}_s$  denote the forward and backward differences.

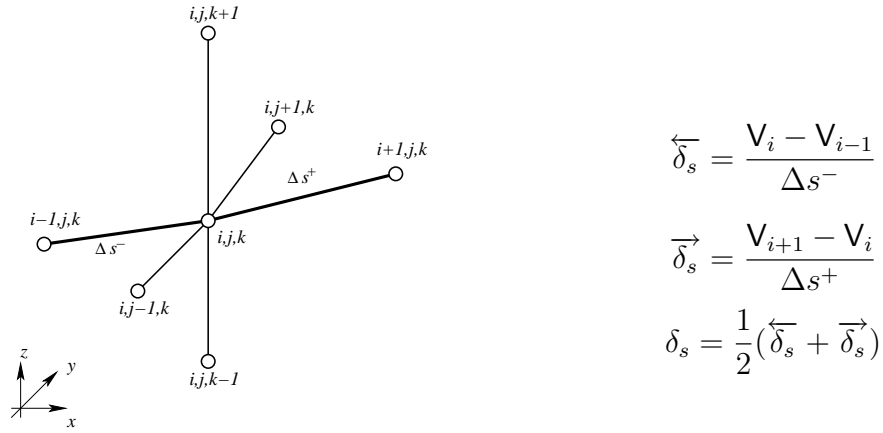


Figure 2: Finite-difference mesh

### Semi-implicit finite-difference scheme

The system of governing equations (1),(2) written here with the additional assumption  $\rho_0 = const$  for simplicity:

$$u_x + v_y + w_z = 0 \tag{6}$$

$$V_t + uV_x + vV_y + wV_z = \underbrace{-\frac{\nabla p}{\rho_0} + [KV_x]_x + [KV_y]_y + [KV_z]_z}_{=RHS} \tag{7}$$

Using the local coordinate transformation described on figure 1 we can rewrite this system so that the continuity equation (6) will take the form:

$$\frac{u_{s1}}{\cos \alpha} + \frac{v_{s2}}{\cos \beta} + w_z - u_z \tan \alpha - v_z \tan \beta = 0 \tag{8}$$

The momentum equations will then be modified to the following form <sup>1</sup>:

$$V_t + \tilde{u}V_{s1} + \tilde{v}V_{s2} + \tilde{w}V_z = \widetilde{RHS} \tag{9}$$

The modified coefficients are defined as follows:

$$\tilde{u} = \frac{u}{\cos \alpha} \quad \tilde{v} = \frac{v}{\cos \beta} \quad \tilde{w} = w - u \tan \alpha - v \tan \beta$$

The right-hand side is transformed in a similar way. The left-hand side of momentum equations is discretized by the following way :

$$V_t \sim \overrightarrow{\delta}_t V_{i,j,k}^n$$

$$\tilde{u}V_{s1} \sim \frac{1}{2} \left( \tilde{u}_{i+1/2}^n \overrightarrow{\delta}_{s1} V_{i,j,k}^n + \tilde{u}_{i-1/2}^n \overleftarrow{\delta}_{s1} V_{i,j,k}^{n+1} \right)$$

<sup>1</sup>The  $\widetilde{RHS}$  and  $\overline{RHS}$  are the modified right-hand sides

$$\begin{aligned}\tilde{v}V_{s_2} &\sim \frac{1}{2} \left\{ \frac{1}{2} \left( \tilde{v}_{j+1/2}^n \overrightarrow{\delta}_{s_2} V_{i,j,k} + \tilde{v}_{j-1/2}^n \overleftarrow{\delta}_{s_2} V_{i,j,k} \right)^n + \right. \\ &\quad \left. + \frac{1}{2} \left( \tilde{v}_{j+1/2}^{n+1} \overrightarrow{\delta}_{s_2} V_{i,j,k} + \tilde{v}_{j-1/2}^{n+1} \overleftarrow{\delta}_{s_2} V_{i,j,k} \right)^{n+1} \right\} \\ \tilde{w}V_z &\sim \frac{1}{2} \left\{ \frac{1}{2} \left( \tilde{w}_{k+1/2}^n \overrightarrow{\delta}_z V_{i,j,k} + \tilde{w}_{k-1/2}^n \overleftarrow{\delta}_z V_{i,j,k} \right)^n + \right. \\ &\quad \left. + \frac{1}{2} \left( \tilde{w}_{k+1/2}^{n+1} \overrightarrow{\delta}_z V_{i,j,k} + \tilde{w}_{k-1/2}^{n+1} \overleftarrow{\delta}_z V_{i,j,k} \right)^{n+1} \right\}\end{aligned}$$

The coefficients  $\tilde{u}$ ,  $\tilde{v}$ ,  $\tilde{w}$  are fixed at the time-level  $n$  in order to linearize locally the system to obtain Oseen-like iterative solver. The combination of different asymmetric space discretization at time levels  $n$  and  $n+1$  allows us to construct finally the numerical scheme that is centered and second order in both space and time. The computational stencil is different for discretization at time level  $n$  and  $n+1$ .

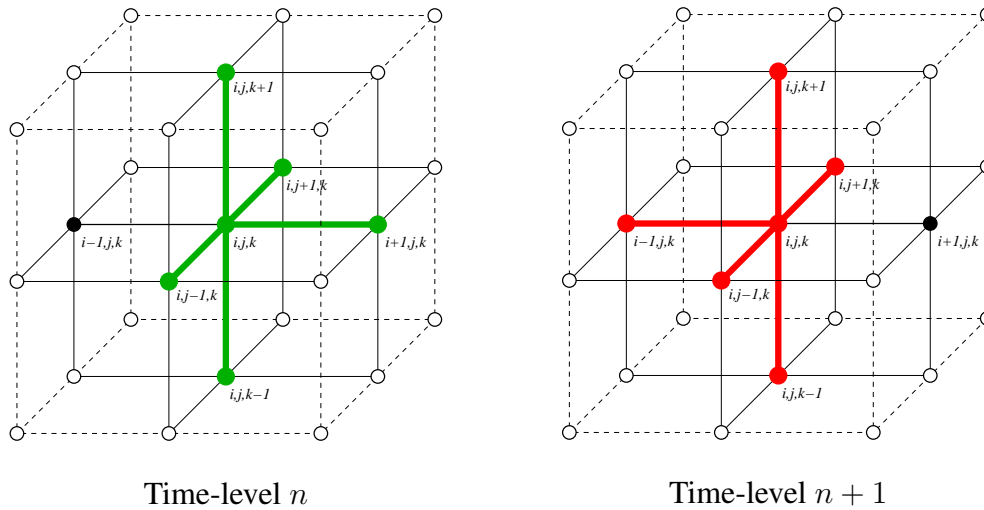


Figure 3: Computational stencil for semi-implicit FD scheme

The dissipative terms on right-hand side are approximated in the same manner. By this discretization we obtain in each column of grid-points the system of linear algebraic equations of the following type:

$$a_1 V_{i,j+1,k}^{n+1} + a_2 V_{i,j,k}^{n+1} + a_3 V_{i,j-1,k}^{n+1} + a_4 V_{i,j,k+1}^{n+1} + a_5 V_{i,j,k-1}^{n+1} = \overline{RHS} \quad (10)$$

This system is solved iteratively in vertical plane  $i = const$ . So the five-diagonal system is converted into three-diagonal.

$$a_5 V_{i,j,k-1}^{\eta+1} + a_2 V_{i,j,k}^{\eta+1} + a_4 V_{i,j,k+1}^{\eta+1} = \overline{RHS} - a_1 V_{i,j+1,k}^{\eta} - a_3 V_{i,j-1,k}^{\eta+1} \quad (11)$$

The  $\eta$  denotes here the iterative index. Usually after  $3 \div 5$  iterations we know the values of  $V = (u, v, w)^T$  with sufficient accuracy. Exactly the same solution scheme can also be used for the scalar transport equations

In the steady (or quasi steady) problems the artificial compressibility method can be used and in such a case the pressure is updated from the modified continuity equation.

$$p_t = -(u_x + v_y + w_z) \quad (12)$$

Also here the above described semi-implicit discretization is used to keep the consistency with the momentum equations solver.

In order to improve the convergency of this method for high Reynolds numbers we add the artificial viscosity terms  $DV_{i,j,k}^n$ . Then we skip to  $(n + 1)$ -th time level and repeat the cycle.

### Artificial viscosity

The combination of artificial dissipation of second and fourth order is used.

$$\begin{aligned}
 DV_i^n &= D^2V_i^n + D^4V_i^n \\
 D^2V_i^n &= \tilde{\epsilon}_2 \Delta x^3 \frac{\partial}{\partial x} |V_x| V_x = \tilde{\epsilon}_2 \Delta x^2 (\epsilon_{i+1/2} V_x - \epsilon_{i-1/2} V_x) \\
 \epsilon_{i+1/2} &= \begin{cases} |V_{i+1} - V_i| & \text{for } |V_{i+1} - V_i| < \frac{K}{10} \\ \frac{K}{10} & \text{for } |V_{i+1} - V_k| \geq \frac{K}{10} \end{cases} \\
 D^4V_i^n &= \tilde{\epsilon}_4 \Delta x^4 V_{xxxx} = \tilde{\epsilon}_4 (V_{i-2}^n - 4V_{i-1}^n + 6V_i^n - 4V_{i+1}^n + V_{i+2}^n)
 \end{aligned}$$

The  $K = \nu + \nu_t$  is coefficient of turbulent diffusion. The coefficients  $\tilde{\epsilon}_2, \tilde{\epsilon}_4 \in \mathbb{R}$  are constants of order  $\Delta x^2$  respectively  $\Delta x^4$ .

### Numerical results

Numerical experiments were performed in a 3D domain of the size  $500 \times 250 \times 400$  meters. The bottom boundary represents a complex terrain orography. The contours of terrain elevation are shown in the following figure 4.

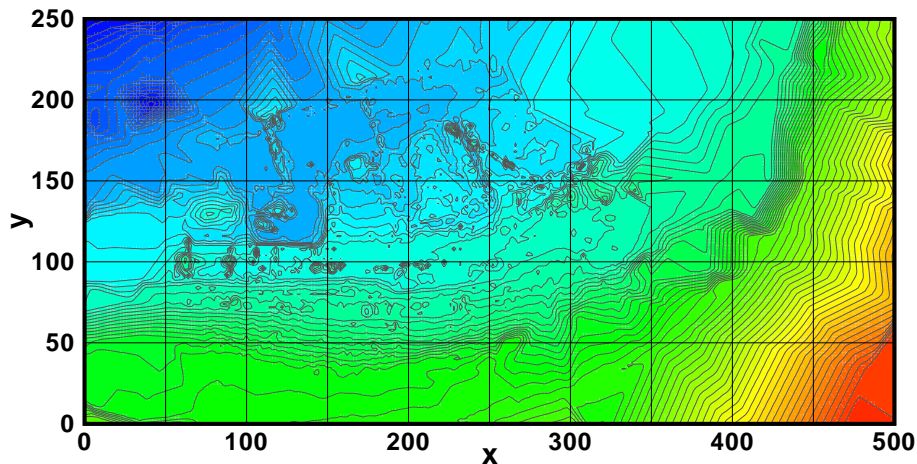


Figure 4: Terrain elevation contours.

The height difference between highest and lowest point of the terrain profile is about 70 meters. The coal storage is represented by a rectangular surface source of pollution. The dimension

of this source is about  $40 \times 20$  meters and is centered at position  $x=125$ ,  $y=120$ . Its location is visible in the figure 5. The wind flow in the model domain is forced by the prescribed velocity profile at the inlet ( $x=0$ ). The maximum velocity  $10\text{m/s}$  is achieved at the upper boundary of the domain.

The figure 5 shows the concentration contours and wind flow streamlines at near-ground level for the basic variant with no obstacles. This variant is used for reference and comparison because it represents the actual state.

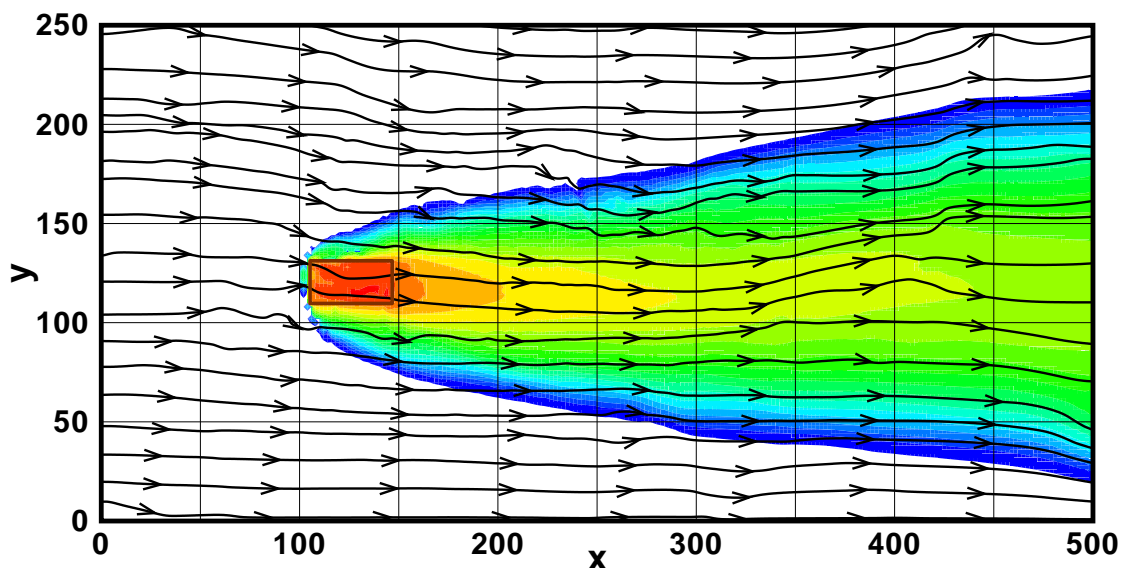


Figure 5: Concentration contours and wind flow streamlines at the near-ground level for the case without obstacles.

In order to slow down and deflect the flow we have placed different obstacles downwind from the simulated source of pollution. The obstacles differ in their shape and size. The first serie of experiments uses an obstacle formed by a block with horizontal projection of the size  $10 \times 60$  meters which is rotated by 45 degrees with respect to mainstream direction. The height of the obstacles varies between 3 and 12 meters. The results of simulations for flow and pollution dispersion for obstacles with heights 3, 6, 9 and 12 meters are shown in the following figures.

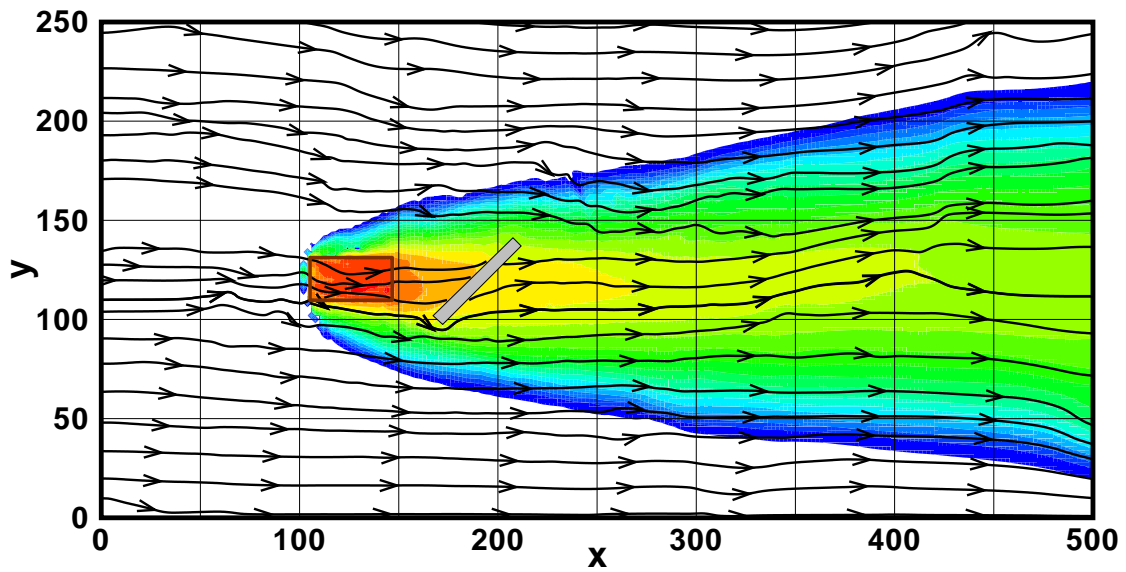


Figure 6: Concentration contours and wind flow streamlines at the near-ground level for the case with obstacle of height 3 meters.

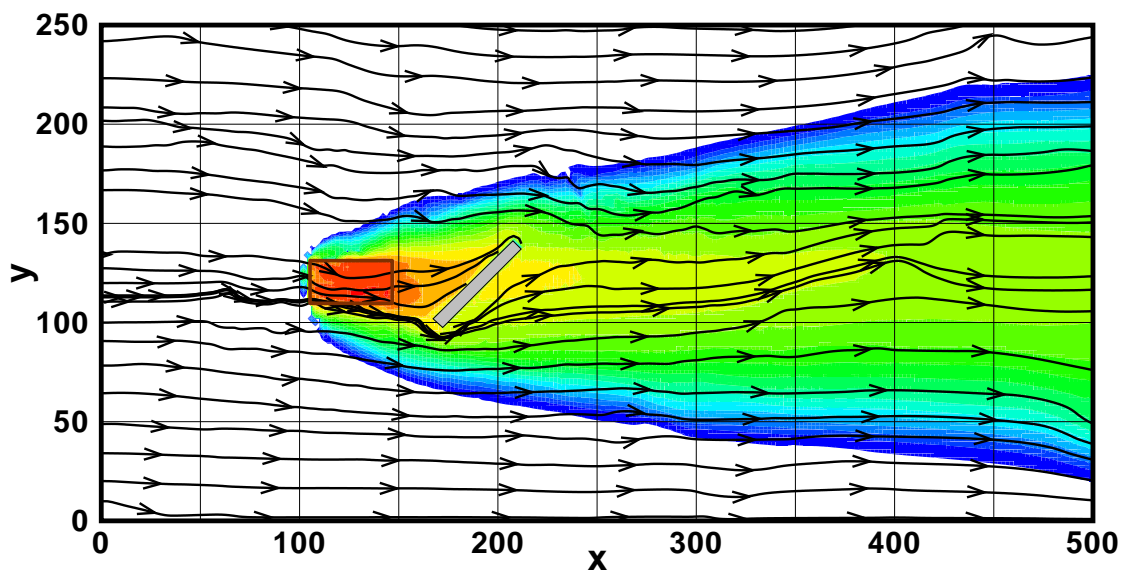


Figure 7: Concentration contours and wind flow streamlines at the near-ground level for the case with obstacle of height 6 meters.

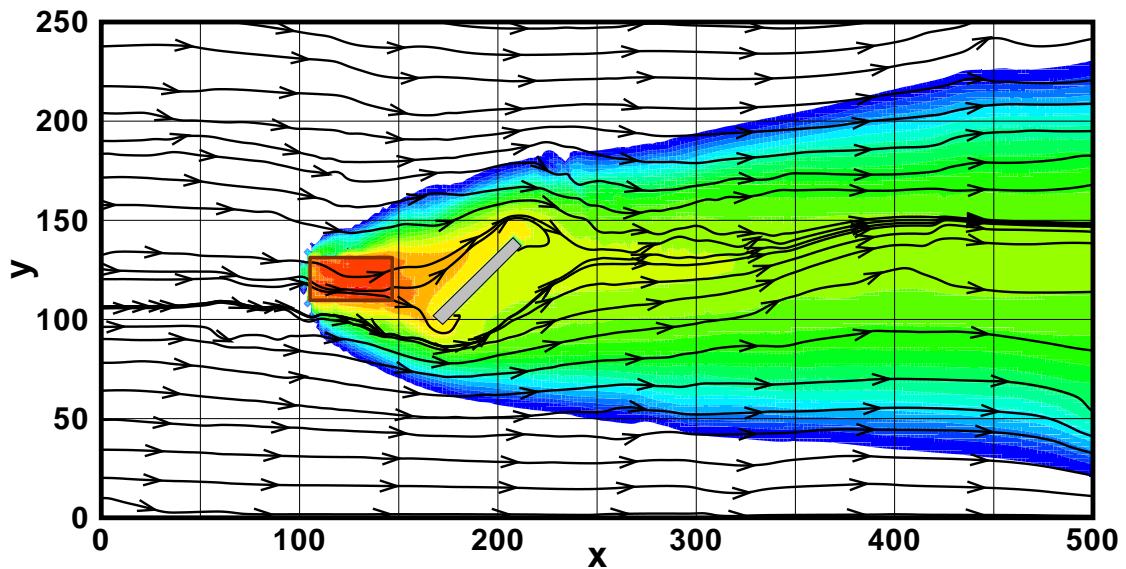


Figure 8: Concentration contours and wind flow streamlines at the near-ground level for the case with obstacle of height 9 meters.

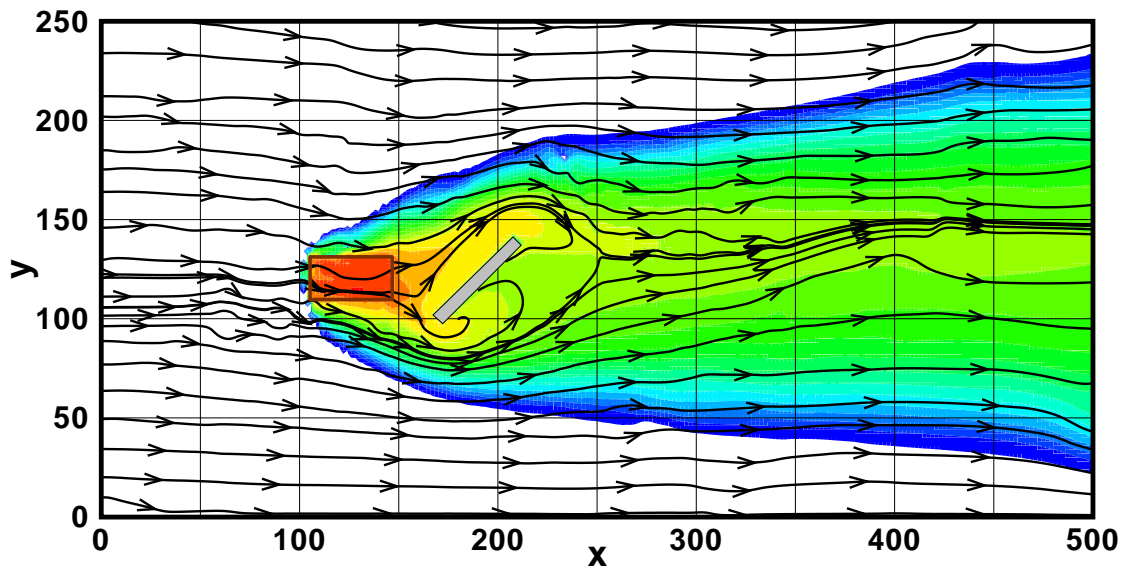


Figure 9: Concentration contours and wind flow streamlines at the near-ground level for the case with obstacle of height 12 meters.

Two other variants have been tested as an attempt to increase the pollution plume deflection. Two obstacles of smaller size and different configuration have been used. In both cases the height of obstacles was 9 meters.



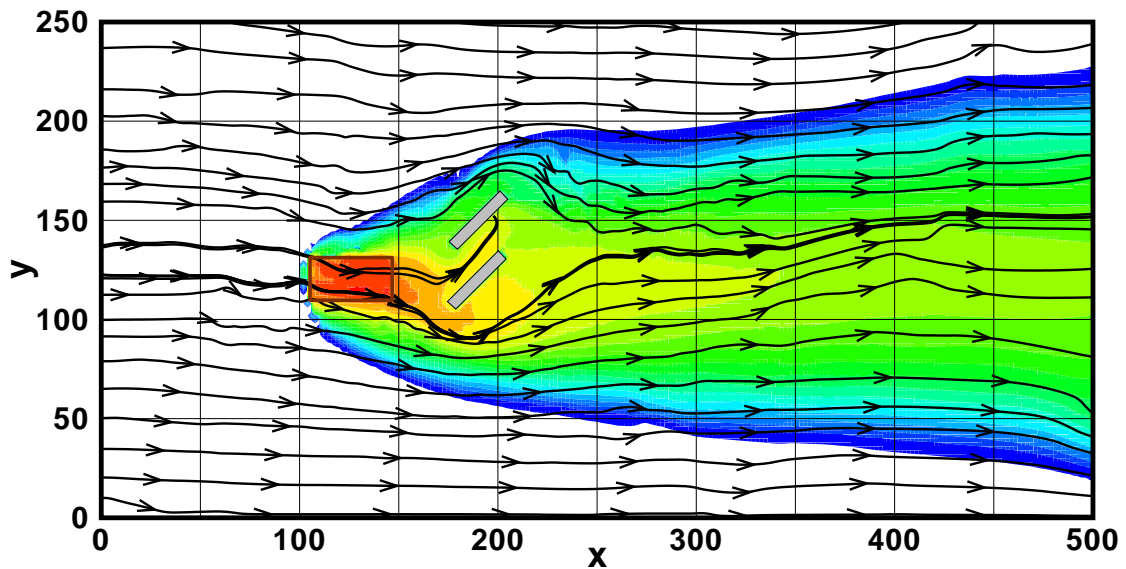


Figure 10: Concentration contours and wind flow streamlines at the near-ground level for the case with two parallel obstacles of height 9 meters.

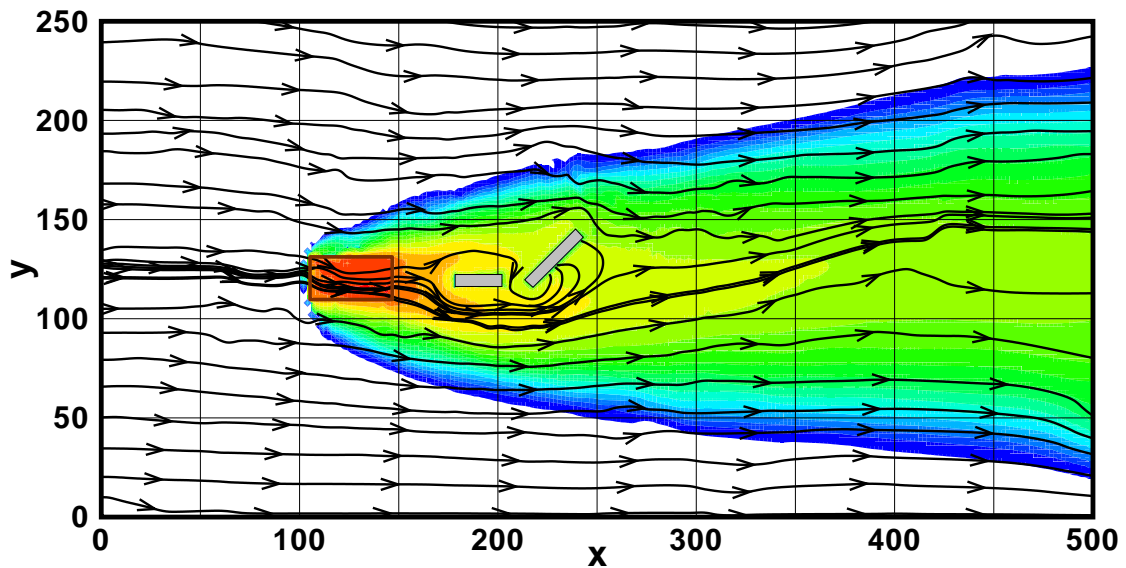


Figure 11: Concentration contours and wind flow streamlines at the near-ground level for the case with two obstacles of height 9 meters.

The simulation results have shown, that the obstacles placed in the proximity of the pollution source have only local impact at both flow field and pollution concentrations. It is necessary to keep in mind that this is only valid for passive pollutant without sedimentation. In order to give

some idea for evaluation of sedimentation we have compared the above mentioned variants of obstacles from the point of view flow speed-up/slow-down at the near-ground level. As the flow slows down, the sedimentation of wind driven particles becomes more significant and thus it is of essential importance to find the regions of decelerated flow. All the variants are compared with the basic variant without obstacles. This allows us to separate the effect of obstacles on flow deceleration.

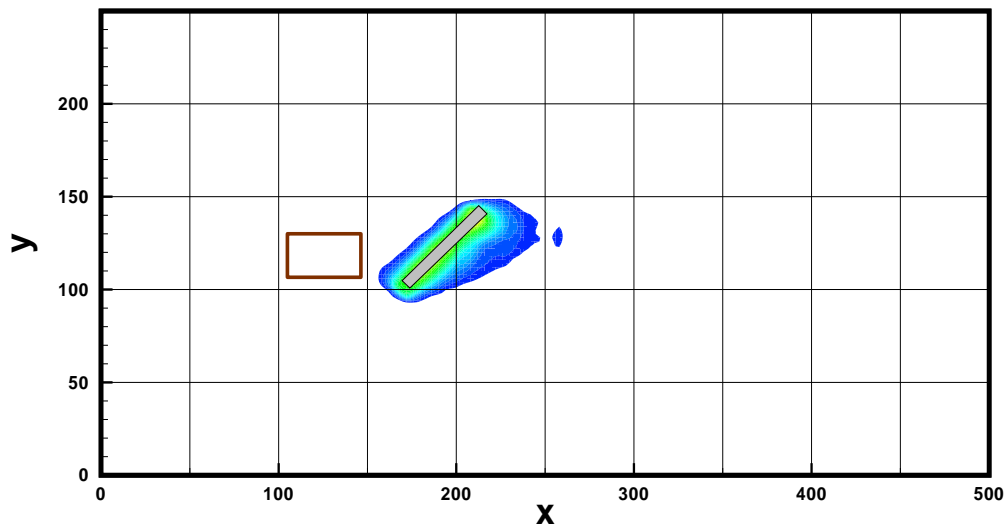


Figure 12: Contours of near-ground wind speed-down for the case of obstacle with height 3 meters with respect to variant with no obstacles.

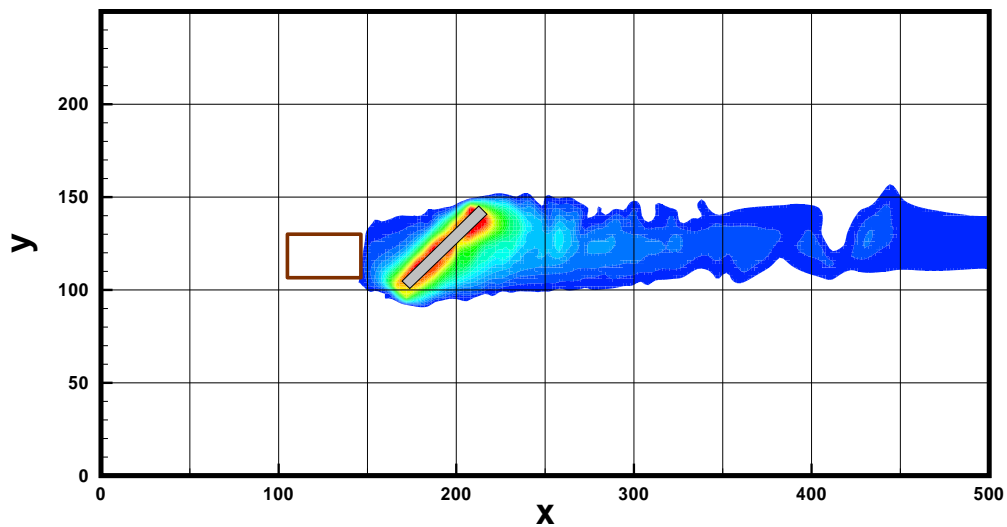


Figure 13: Contours of near-ground wind speed-down for the case of obstacle with height 6 meters with respect to variant with no obstacles.

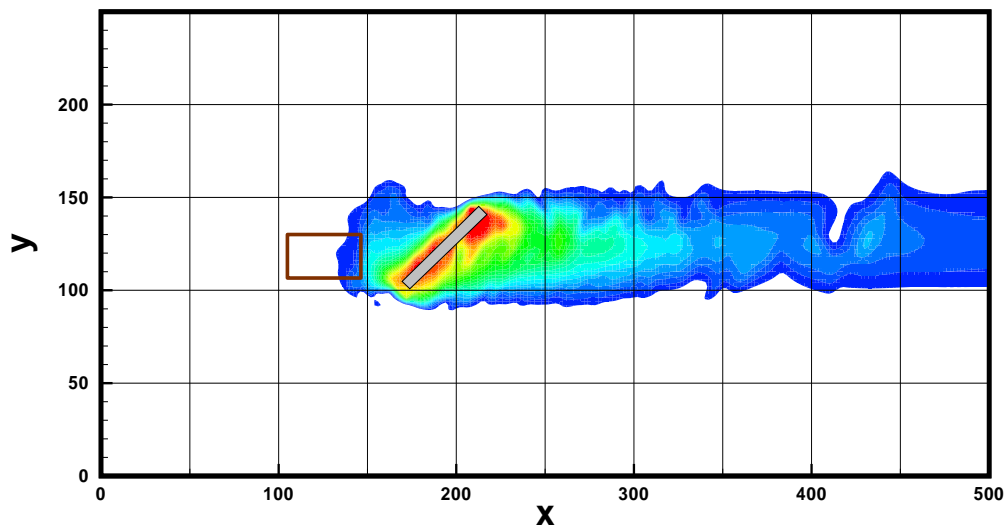


Figure 14: Contours of near-ground wind speed-down for the case of obstacle with height 9 meters with respect to variant with no obstacles.

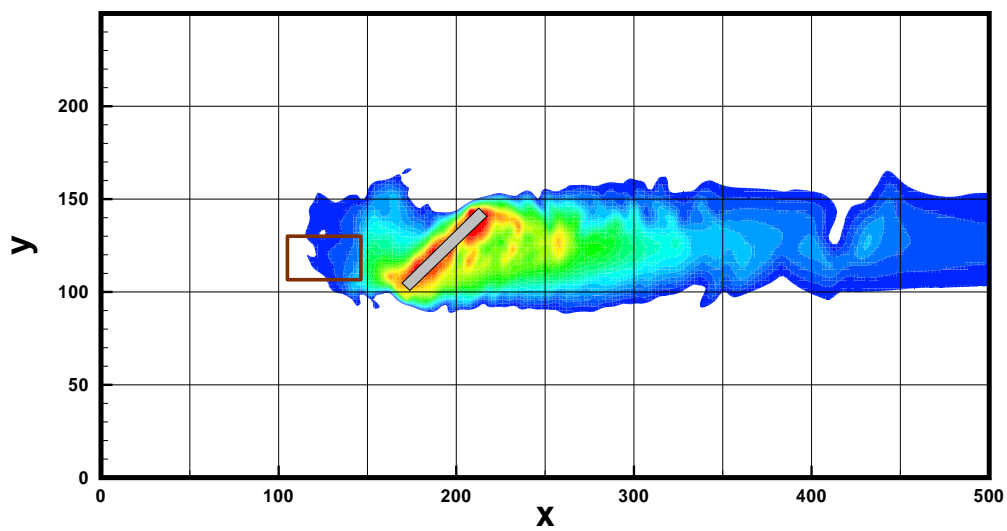


Figure 15: Contours of near-ground wind speed-down for the case of obstacle with height 12 meters with respect to variant with no obstacles.

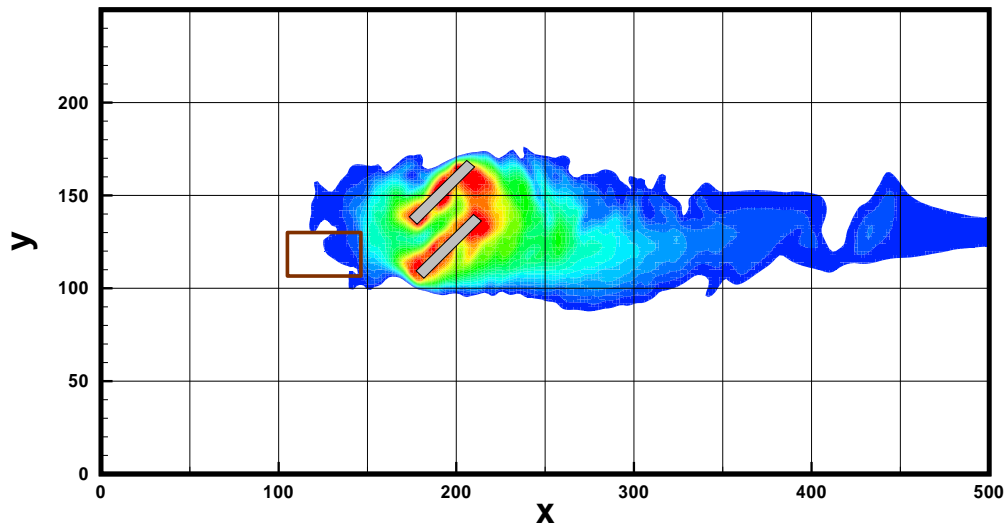


Figure 16: Contours of near-ground wind speed-down for the case of two parallel obstacles with height 9 meters with respect to variant with no obstacles.

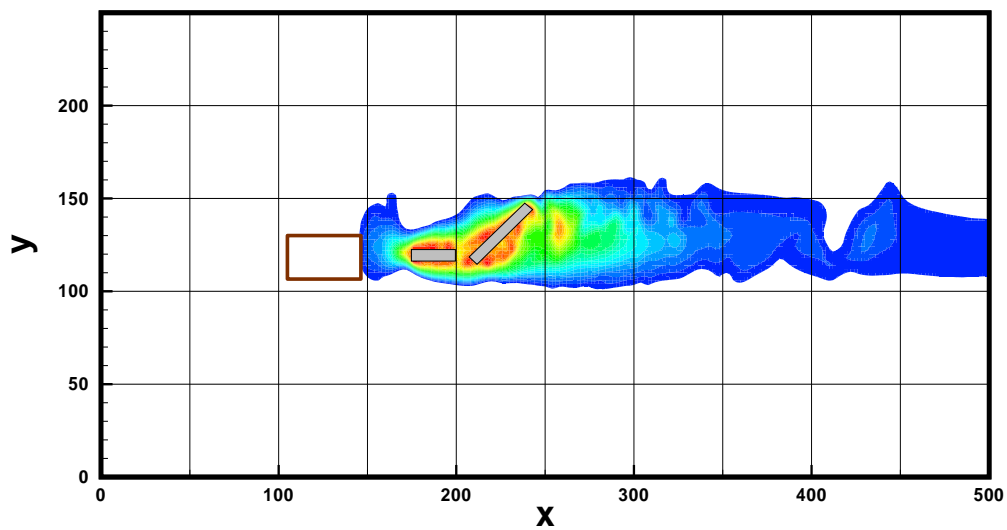


Figure 17: Contours of near-ground wind speed-down for the case of two obstacles with height 9 meters with respect to variant with no obstacles.

## Conclusions, remarks

From the presented tests it is possible to draw the following conclusions:

- The selected mathematical model is able to describe properly the pollution dispersion problems in complex terrain.

- The numerical method used to solve the set of governing equations seems to be sufficiently robust and efficient for the appropriate resolution of given class of problems.
- The presented numerical simulations have shown that the effect of simulated obstacles on the flow and pollution dispersion has only local impact on both velocity and concentration field. This is caused mainly by the complexity of the terrain, where the orography profile involves height changes with scales much larger than the maximum height of the simulated obstacles. Thus the orography effect is dominant in this case.
- More detailed study of dust sedimentation should be performed in order to quantify the effects of obstacles on deposition of particles of different sizes.

### Acknowledgment

The financial support for the present project was partly provided by the *Grant No. IET400760405* and by the Research Plan *MSM 6840770010* of the *Ministry of Education of Czech Republic*.

### References

- [1] BENEŠ, L., BODNÁR, T., FRAUNIÉ, P., & KOZEL, K.: Numerical Modelling of Pollution Dispersion in 3D Atmospheric Boundary Layer. In: *Air Pollution Modelling and Simulation* (edited by B. SPORTISSE), (pp. 69–78). Springer Verlag (2002).
- [2] BODNÁR, T., KOZEL, K., FRAUNIÉ, P., & BENEŠ, L.: Numerical Modelling of Pollution Dispersion in Complex Terrain. In: *Air Pollution IX.*, (pp. 85–94). WIT Press (2001).
- [3] BODNÁR, T., KOZEL, K., FRAUNIÉ, P., & JAŇOUR, Z.: Numerical Simulation of Flow and Pollution Dispersion in 3D Atmospheric Boundary Layer. *Computing and Visualization in Science*, vol. 3, no. 1–2: (2000) pp. 3–8.
- [4] BODNÁR, T., KOZEL, K., FRAUNIÉ, P., & JAŇOUR, Z.: Simulation of Flow and Pollution Dispersion in 3D Atmospheric Boundary Layer. *Computing and Visualization in Science*, vol. 3, no. 1–2.